Evolution of the melt source during protracted crustal anatexis; an example from the Bhutan Himalaya

Thomas Hopkinson[1], Nigel Harris[1*], Nick M W Roberts[2] Clare Warren[1], Sam Hammond[1], Christopher J Spencer[3], Randall R Parrish[2,4]

[1]School of Environment, Earth and Ecosystem Sciences, Open University, Milton Keynes, MK7 6AA, UK

[2] NERC Isotope Geosciences Laboratory, British Geological Survey, Keyworth, NG12 5GG, UK

[3]Earth Dynamics Research Group, TIGeR (The Institute of Geoscience Research), School of Earth and Planetary Sciences, Curtin University, Perth, Australia

[4]Current address: School of Earth and Environmental Sciences, University of Portsmouth, Portsmouth PO1 2UP, UK

[*] n.b.w.harris@open.ac.uk

ABSTRACT

The chemical compositions of growth zones of magmatic zircon provide powerful insight into evolving magma compositions due to their ability to record both time and the local chemical environment. *In situ* U-Pb and Hf isotope analyses of zircon rims from Tertiary leucogranites of the Bhutan Himalaya reveal, for the first time, an evolution in melt composition between 32-12 Ma. The data indicate a broadly stable melt source from 32 Ma to 17 Ma, and the progressive addition of an older source component to the melt from at least ~17 Ma, and possibly from as early as 21 Ma. Age-corrected εHf ratios decrease from between -10 to -15 down to values as low as -23 by 12 Ma. Complementary whole-rock Nd isotope data corroborate the Hf data, with a progressive decrease in $\varepsilon Nd_{(T)}$ from ~18 to 12 Ma. Published zircon and whole-rock Nd data from different lithotectonic units in the Himalaya suggest a chemical distinction between the younger Greater Himalayan Series (GHS) and the older Lesser Himalaya Series (LHS). The time-dependent isotopic evolution shown in the leucogranites demonstrates a progressive increase in melt contribution from older lithologies, indicative of increasing LHS involvement in Himalayan melting over time. The time-resolved data therefore are consistent with a model wherein LHS material was incorporated into the base of the hanging wall of the Main Central thrust from ~17 Ma. Exhumation of this hanging wall material along the thrust triggered decompression melting under fluid-absent conditions during the later stages of orogenesis.

INTRODUCTION

Crustal melting is a fundamental process both for chemical differentiation and for facilitating ductile deformation of the Earth's continental crust. In the Himalaya, Late Oligocene-Miocene leucogranites provide a well-documented example of crustal melting induced by continental collision. Oxygen and hafnium isotope data from Himalayan leucogranite zircon rims demonstrate that these granites are examples of pure crustal melting with no detectable mantle input (Hopkinson et al., 2017). The timeframe across which melting has occurred along the Himalaya orogen ranges from at least 25 Ma to 9 Ma (Guo and Wilson, 2012), although granites as old as 39 Ma has been identified in the western Himalaya (Prince et al., 2001). Despite this extensive period of regional anatexis, no time-dependant change in the magmatic source has been recognised thus far. The evolving thermal regime during collisional orogenesis should lead to migration of melt source regions, and involvement of sources from different crustal levels. In the case of the Himalayan leucogranites it is possible that the apparent absence of time-dependent trends results from the lack of chronological resolution using traditional whole-rock isotopic data. The importance of recognising the temporal evolution of melt zones lies in better constraining models of thermal and structural evolution of the continental crust during orogenesis. Here we evaluate the Hf isotope composition of zircon sampled from leucogranites in Bhutan (Eastern Himalaya), along with new whole-rock Nd isotope data. The temporal changes observed in isotopic composition provides, for the first time, direct evidence for a time-dependant change in the mid-crustal material undergoing melting during Himalayan crustal thickening.

REGIONAL SETTING

We have analysed the isotopic composition of zircon from peraluminous Oligocene to Miocene leucogranites exposed in the eastern Himalayan orogen in Bhutan (Fig.1). The granites represent a range of mineralogical types, including seven two-mica (1G03, 3A03, 4D01, 1247, 1251, CWB16 and CWB23), two tourmaline-bearing (1G02, 1215), two garnet-bearing (1D01, 3A02) and one pegmatitic two-mica (1G01) leucogranite. Across the orogen, such granites intrude upper amphibolite-facies metasediments of primarily Neoproterozoic source age, the Greater Himalayan Sequence (GHS; Ahmad et al., 2000; Gehrels et al., 2011). In Bhutan, the leucogranites are emplaced in the uppermost lithologies of the GHS, close to or crossing the tectonic boundary with the Tethyan sediments (Greenwood et al., 2016) as is evident from Fig. 1. Structurally below the GHS, and underthrust along the Main Central thrust (MCT), is the Lesser Himalayan Sequence (LHS), a primarily Paleoproterozoic-sourced stack of metasediments (Ahmad et al., 2000; Gehrels et al., 2011). Both the GHS and LHS comprise a mix of pelitic, orthogneiss, carbonate and quartzite compositions. The pelitic assemblages are significantly the most melt-fertile, and therefore provide appropriate source materials for anatectic melts at temperatures below ~760ºC (at pressures equivalent to melting in the mid to lower crust; Patiño Douce and Johnston, 1991).

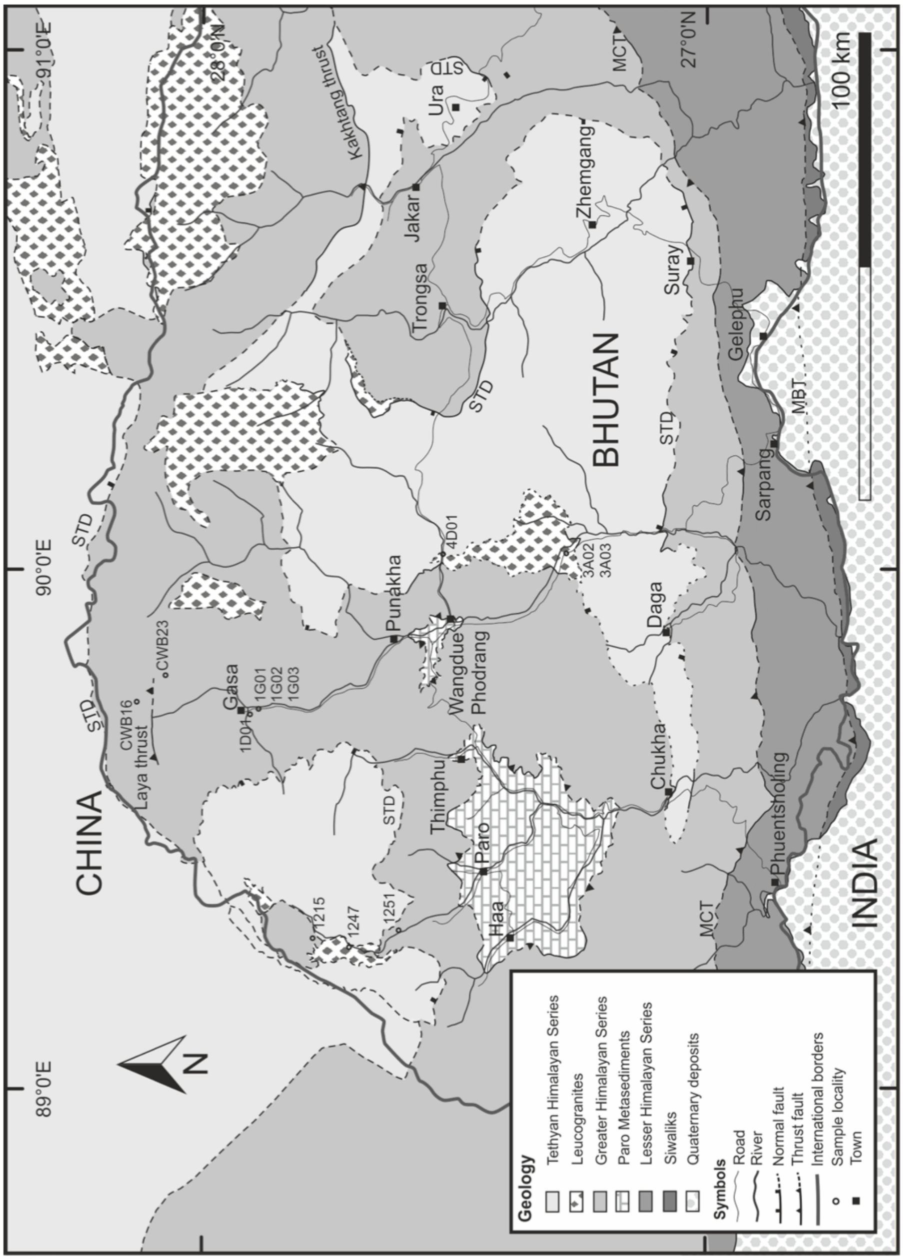

Figure 1. Geological map of western and central Bhutan, adapted from Greenwood et al. (2016), showing sample localities. STD = South Tibetan Detachment, MCT = Main Central Thrust, MBT = Main Boundary Thrust, MFT = Main Frontal Thrust.

Whole-rock isotope geochemical data from equivalent High Himalayan leucogranites exposed across the Himalayan orogen suggest that they formed largely by partial melting of the pelitic lithologies of the GHS into which the granites intrude (Le Fort et al., 1987; Harris and Massey, 1994; Hopkinson et al., 2017). However, a whole-rock Sr–Nd isotope study has suggested that a small contribution from LHS-derived fluids has also contributed to some leucogranite melts (Guo and Wilson, 2012). Critically, there is no observed temporal control on the proposed inputs from the LHS. Our new zircon rim U-Pb and age-corrected εHf isotope analyses coupled with whole-rock Nd isotope data show that, at least in Bhutan, there is progressive increase in melt contribution from the LHS after ~17 Ma.

METHODS

Zircon U-Pb and Lu-Hf isotope methods and data were previously reported in Hopkinson et al. (2017). Whole-rock Sm-Nd isotope analyses were obtained at the Open University (UK) by thermal ionization mass spectrometry. Further methodological details and the full dataset is provided in the supplementary information.

RESULTS

Zircon from all twelve samples provided rims of Tertiary age ranging from 34 to 11 Ma (Fig. 2, Table DR1), and the majority have inherited cores of Early Paleozoic or Proterozoic age. The complete dataset is presented in Hopkinson et al. (2017). Zircon from individual samples record growth over protracted periods, with spans in individual zircon ages ranging from 0.9 to 15.5 Ma (Fig. 2).

This spread of ages from individual hand-samples is typical of Himalayan and other S-type granites (Lederer et al., 2013), and the apparent longevity of melt formation has been ascribed to protracted timescales of zircon crystallisation and long magma residence times (Farina et al., 2018) and more specifically in the Himalaya to episodic pulse melting of 1-2 Ma duration (Lederer et al., 2013).

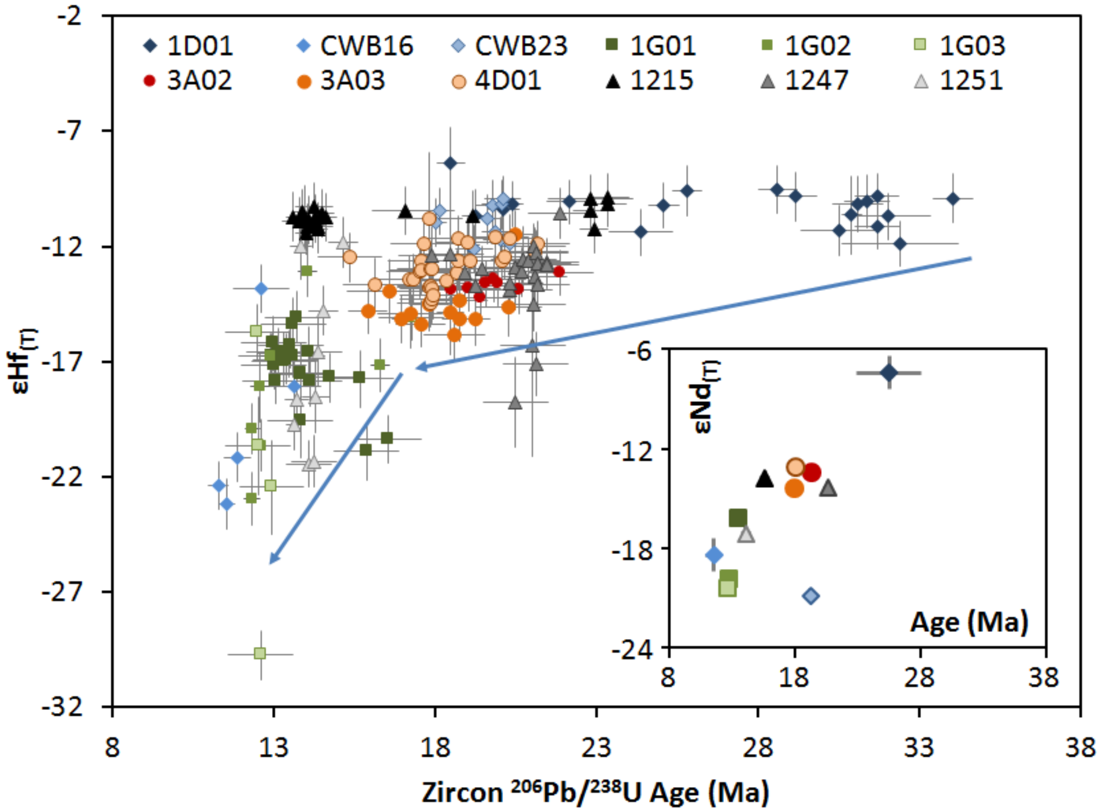

Figure 2. Zircon rim U–Pb age versus εHf$_{(T)}$. Data from Hopkinson et al. (2017) and Table DR1. Error bars are 2σ. Inset shows U–Pb age versus εNd$_{(T)}$. Data from Table DR2.

Hafnium isotopic compositions are plotted against their corresponding zircon age in Fig. 2. Age corrected isotope ratios (εHf$_{(T)}$) range from -8.4 to -29.8. Some granite samples preserve large differences in the Hf isotopic composition of the zircon rims (e.g. samples 1G03 and 1247). This is likely a result of the lack of homogenisation in the evolving magma, a characteristic that has been documented in whole-rock studies of Himalayan leucogranites (Deniel et al., 1987) and may be attributed to high melt viscosities of low-temperature, H_2O-undersaturated siliceous magmas (Harris et al., 2000). Variability in Hf isotope compositions at the hand-sample scale can also be linked to disequilibrium melting and different mineral phases hosting different reservoirs of radiogenic Hf (Farina et al., 2014; Tang et al., 2014).

Our data show a distinct secular change in $\varepsilon Hf_{(T)}$ values, with increasingly lower values in younger samples. Specifically, the zircon compositions show a change in source, or in the balance between contributing sources, that is initiated between 21 and 17 Ma. We note that the marked change occurs after 17 Ma, but outlying data (sample 1247) suggest hints of earlier change at 21 Ma. After 17 Ma, the population of all but one sample (1215) decreases to $\varepsilon Hf_{(T)} < -16$. In terms of two-stage model ages for these zircons, zircon rims older than 17 Ma have model ages of 1520 to 2000 Ma, whereas those after 17 Ma range from 2000 to 2620 Ma.

Whole-rock $\varepsilon Nd_{(T)}$ ratios range from -7.4 to -20.9 (Fig. 2 inset). There is a general decreasing trend through time across eleven of the twelve samples. This trend broadly correlates with the *in-situ* zircon εHf data, except for sample CWB23 that has a low εNd ratio. Assuming that the whole-rock data comprises a complete dissolution of all minerals, and because the εHf data fit the broad array exhibited by all samples, this sample points to a sample-specific disequilibrium behaviour in the Sm-Nd system.

DISCUSSION

An Evolving Magma Source

Previous studies implicate the GHS as the dominant source for Himalayan leucogranite melts (Harris and Massey, 1994; Guo and Wilson, 2017; Hopkinson et al., 2017). To address the possible cause of the evolving isotopic signature of the Bhutanese leucogranites in terms of source rocks, we compare our new zircon-derived data with existing whole-rock Nd and Hf isotope data from the Himalayan metasedimentary formations. Previous studies have described a clear distinction between GHS and LHS units in terms of their isotopic signature, for example, whole-rock Nd data taken from across the MCT in Sikkim (Mottram et al., 2014), indicates εNd values of -12.1 to -18.3 in the GHS (hanging wall), and -23.4 to -27.7 in the LHS (footwall). These overlap directly with the ranges obtained from metasedimentary formations in Bhutan of εNd -12.1 to -17.6 for the GHS and -25.9 to -32.3 for the LHS (Richards et al., 2006). Whole-rock Nd isotope data for the samples in this study (Fig. 2, inset) have values of $\varepsilon Nd_{(T)}$ ranging from -7.4 to -20.9, thus, the entire data array can broadly be generated from GHS source rocks, but the lower values are compatible with an increasing LHS component. The recognition of multiple sources for long-duration anatectic melts is well established in previous zircon studies (Farina et al., 2018).

A plot of our *in-situ* zircon Hf isotope data vs. age is shown in Fig. 3 against data compiled from across the GHS and LHS (Spencer et al., 2018). The compiled data show that the GHS yields a broad range in $\varepsilon Hf_{(17)}$ values, from -8 to -30, with a dominant population between -8 to -18. The LHS mainly falls between $\varepsilon Hf_{(17)}$ -21 and -35. A boundary between GHS and LHS could be inferred around $\varepsilon Hf_{(17)}$ -22. As with the Nd isotope data, the leucogranite data can be generated by derivation from a GHS source, but also indicate an increasing LHS (or at least older) source through time.

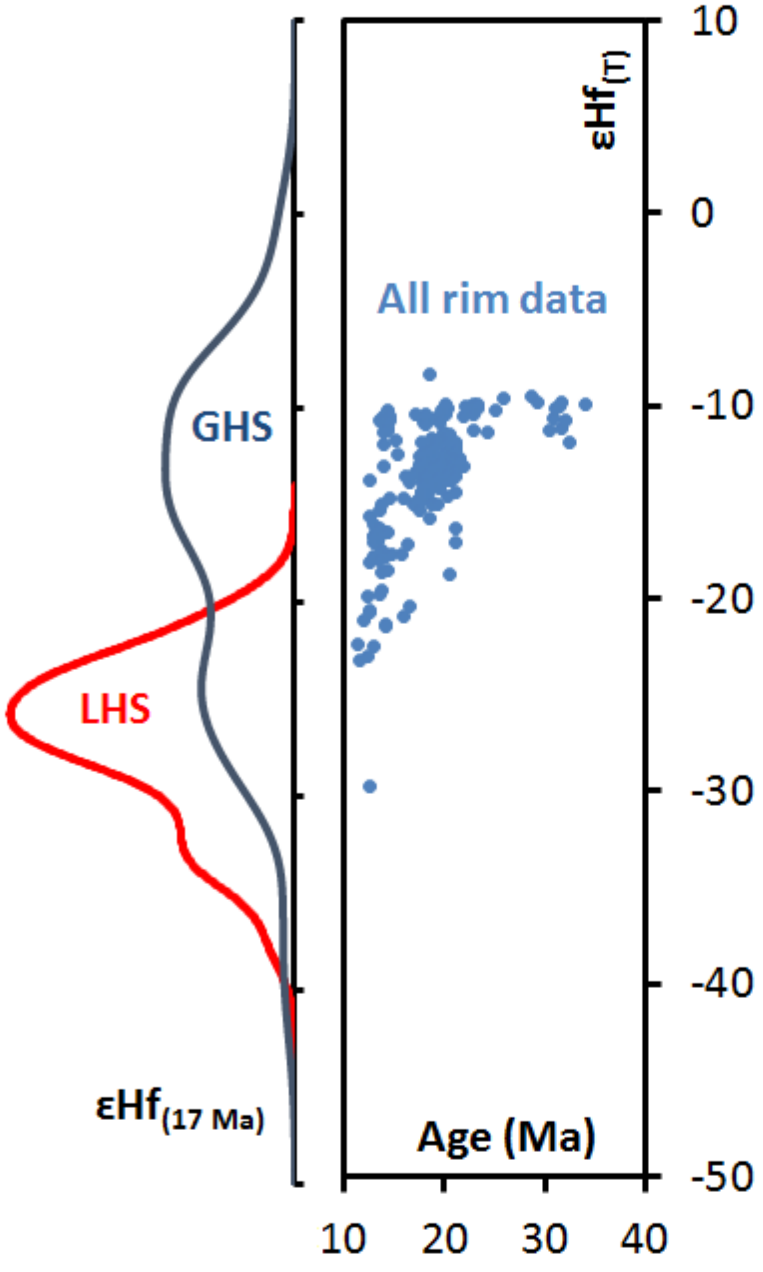

Figure 3. Zircon rim U-Pb-Hf data from Figure 2 shown with Kernel Density Estimates of GHS and LHS detrital zircon data, recalculated at 17 Ma, based on the compilation of Spencer et al. (2018).

In addition, the dataset of Hopkinson et al. (2017) shows that samples with 1800–1900 Ma zircon cores are only found in samples with younger zircon rims (Table DR2; Fig. DR2). This Paleoproterozoic orogenic event uniquely affected the LHS (Ahmad et al., 2000; Kohn et al., 2010), given that the GHS was not deposited until the Neoproterozoic (Richards et al., 2006; Spencer et al., 2012). Taken together, the isotopic evidence from zircon rims and whole-rock data, and the age of zircon cores, strongly suggest that an increasing component of older and more radiogenic material was being melted during the period of anatexis from 17 Ma and possibly from as early as 21 Ma.

Given that the available melt-fertile (i.e. pelitic) source material is restricted to two Himalayan formations (LHS and GHS) and that the GHS into which the granites are emplaced is underthrust by the LHS (Heim and Gansser, 1939), then the results from this study provide clear evidence for a GHS-sourced melt zone in the Oligocene, and subsequent tectonic or thermal evolution to allow some melting of the LHS during the early Miocene (since 17 Ma, and possibly 21 Ma). Direct evidence of melting in the LHS is yet to be recognised from exposed lithologies in the MCT zone, but kyanite-grade LHS schists have been identified that have reached temperatures of ~640ºC, sufficient for melting to occur in fertile lithologies (Caddick et al., 2007).

Tectonic Implications

The key finding of this study is that increasing components of older material are incorporated into the anatectic melt from at least 17 Ma. Whilst the data presented here do not define a unique tectonic model for the evolution of the Himalaya, they do require that the pelitic sediments of the LHS are subjected to melting from the early Miocene during a period of rapid exhumation. For exhumation to cause melting, the melt reaction must be characterised by a positive gradient of the granite solidus, which in turn requires fluid-absent melting (Harris and Massey, 1994). The Himalayan leucogranites provide a classic example of fluid-absent muscovite melting, as indicated by their trace-element geochemistry (Inger and Harris, 1993); more recently, some examples of fluid-present melting have also been documented in the Himalaya (Gao et al., 2017; Huang et al., 2017). The trace-element characteristics of the granites in this study are indicative of fluid-absent melting (Fig. 4). There is no perceptible systematic difference in either element chemistry (Table DR3) or mineralogy between granites with older or younger source regions; each group includes both peraluminous two-mica and tourmaline-bearing assemblages. These observations, coupled with empirical thermobarometric evidence for exhumation of the GHS in the eastern Himalaya at the time of melt formation (~16 Ma) at a rate of 2±1 mm yr^{-1} (Harris et al., 2004), suggest that melting in Bhutan was induced by decompression during exhumation.

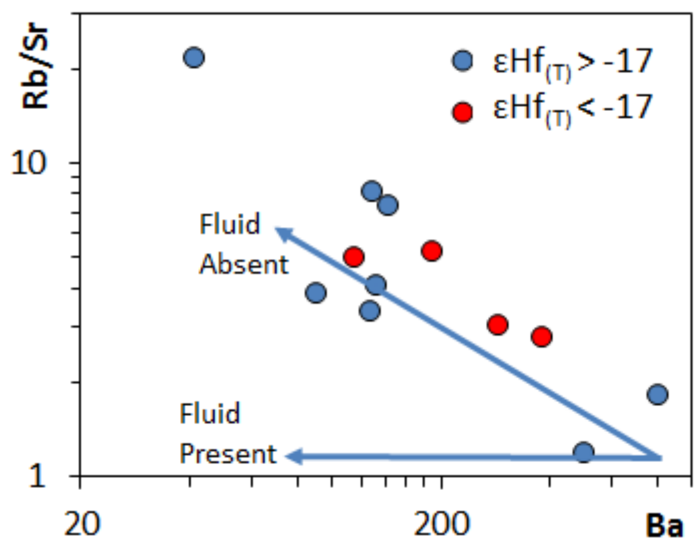

Figure 4. Leucogranite Rb/Sr versus Ba plot. Samples are split by their weighted mean $\varepsilon Hf_{(T)}$ values. Modelled trends are shown for fluid-absent and fluid-present melting (Inger and Harris, 1993).

A recent geochemical study of the ~5 km thick MCT zone in Sikkim argued for progressive tectonic accretion of Lesser Himalayan material from the footwall to the hanging wall of the MCT as it progressively cut structurally downwards from ~17 Ma (Mottram et al., 2015; their Fig. 12), a scenario based on the kinematic model of Bollinger et al. (2006). Metamorphism in the MCT zone developed as heat advected downward from the overriding GHS material. Following such accretion, exhumation along the hanging wall of the thrust could have led to decompression melting of both GHS and accreted LHS material. The introduction of LHS-sourced material into the melt zone may therefore mark the initiation of accretion of the LHS into the hanging wall of the thrust. It is probable that, irrespective of the precise cause of a changing melt source around the MCT, melting will have enabled continued movement along this key Himalayan structure through reducing the mechanical strength of anatectic rocks around the thrust zone.

CONCLUSIONS

In-situ LA-ICP-MS analyses of zircon rims from Himalayan leucogranites provide the first evidence for secular compositional change of melts generated by protracted anatexis during the late Oligocene to mid Miocene. Increasing components from older source regions from 21-17 Ma to 12 Ma requires increased melting of LHS material during this period. Rapid exhumation of the hanging wall of the MCT is well documented through the Miocene, and the granites from the eastern Himalaya provide trace-element characteristics indicative of fluid-absent melting. A tectonic model that is consistent with all observations is one in which older LHS material was accreted to the hanging wall of the MCT, and thus the base of the GHS, during the progressive evolution of the structure.

ACKNOWLEDGEMENTS

T.H. acknowledges funding from NERC CASE studentship NE/K501074/1. C.W. acknowledges funding from NERC Advanced Fellowship NE/HO16279/1. Analytical work was funded by NERC facility grants IMF478/0513 and IP1403/111. Thanks are extended to D. Regis and D. Young for field assistance, A. Wood for assistance with sample preparation at NIGL, and T. Argles, B. Charlier, D. Regis and C. Mottram for fruitful discussions.

REFERENCES CITED

Ahmad, T., Harris, N., Bickle, M., Chapman, H., Bunbury, J., and Prince, C., 2000, Isotopic constraints on the structural relationships between the lesser Himalayan series and the high Himalayan crystalline series, Garhwal Himalaya: Geological Society of America Bulletin, v. 112, p. 467–477.

Bollinger, L., Henry, P., and Avouac, J., 2006, Mountain building in the Nepal Himalaya: Thermal and kinematic model: Earth and Planetary Science Letters, v. 244, p. 58–71, https://doi.org/10.1016/j.epsl.2006.01.045.

Caddick, M.J., Bickle, M.J., Harris, N.B.W., Holland, T.J.B., Horstwood, M.S.A., Parrish, R.R., and Ahmad, T., 2007, Burial and exhumation history of a Lesser Himalayan schist: Recording the formation of an inverted metamorphic sequence in NW India: Earth and Planetary Science Letters, v. 264, p. 375–390, https://doi.org/10.1016/j.epsl.2007.09.011

Deniel, C., Vidal, P., Fernandez, A., Le Fort, P., and Peucat, J.J., 1987, Isotopic study of the Manaslu granite (Himalaya, Nepal): inferences on the age and source of Himalayan leucogranites: Contributions to Mineralogy and Petrology, v. 96, p.78–92.

Farina, F., Stevens, G., Gerdes, A., and Frei, D., 2014. Small-scale Hf isotopic variability in the Peninsula pluton (South Africa): the processes that control inheritance of source $^{176}Hf/^{177}Hf$ diversity in S-type granites: Contributions to Mineralogy and Petrology, v. 168, p.1065, https://doi.org/10.1007/s00410-014-1065-8.

Farina, F., Dina, A., Ovtcharova, M., Davies, J.H.F.L., Greber, N.D., Bouvier, A.S., Baumgartner, L., Ulianov, A., and Schaltegger, U., 2018. Zircon petrochronology reveals the timescale and mechanism of anatectic magma formation: Earth and Planetary Science Letters, v. 495, p. 213–223, https://doi.org/10.1016/j.epsl.2018.05.021.

Gao, L.E., Zeng, L., and Asimow, P.D., 2017. Contrasting geochemical signatures of fluid-absent versus fluid-fluxed melting of muscovite in metasedimentary sources: The Himalayan leucogranites: Geology, v. 45, p.39-42, https://doi.org/10.1130/G38336.1.

Gehrels, G.P., Kapp, P., DeCelles, A., Pullen, R., Blakey, A., Weislogel, A., Ding, L., Duynn, J., Martin, A., McQuarrie, N., and Yin, A. 2011, Detrital zircon geochronology of pre-Tertiary strata in the Tibetan-Himalayan orogen: Tectonics, v. 30, no. 5,. doi:10.1029/2011TC002868.

Greenwood, L.V., Argles, T.W., Parrish, R.R., Harris, N.B.W., and Warren, C., 2016, The geology and tectonics of central Bhutan: Journal of the Geological Society, v. 173, p. 215–238, https://doi.org/10.1144/jgs2015-031.

Guo, Z., and Wilson, M., 2012, The Himalayan leucogranites: constraints on the nature of their crustal source region and geodynamic setting: Gondwana Research, v. 22, p. 360–376, https://doi.org/10.1016/j.gr.2011.07.027.

Harris, N., and Massey, J., 1994, Decompression and anatexis of Himalayan metapelites: Tectonics, v. 13, p. 1537–1546, https://doi.org/10.1029/94TC01611.

Harris, N., Vance, D., and Ayres, M., 2000, From sediment to granite: timescales of anatexis in the upper crust: Chemical Geology, v. 162, p.155–167, https://doi.org/10.1016/S0009-2541(99)00121-7.

Harris, N.B.W., Caddick, M., Kosler, J., Goswami, S., Vance, D., and Tindle, A.G., 2004, The pressure-temperature-time path of migmatites from the Sikkim

Himalaya: Journal of Metamorphic Geology, v. 22, p. 249–264, https://doi.org/10.1111/j.1525-1314.2004.00511.x.

Heim, A., and Gansser, A., 1939, Central Himalaya: Geological Observations of the Swiss Expedition, 1936: Memoires de la Société Helvetique des Sciences Naturelles, v. 73.

Hopkinson, T.N., Harris, N.B.W., Warren, C.J., Spencer, C.J., Roberts, N.M.W., Horstwood, M.S.A., Parrish, R.R., and EIMF, 2017, The identification and significance of pure sediment-derived granites: Earth and Planetary Science Letters, v. 467, p. 57–63, https://doi.org/10.1016/j.epsl.2017.03.018.

Huang, C., Zhao, Z., Li, G. and Zhu, D.C., Liu, D., and Shi, Q., 2017, Leucogranites in Lhozag, southern Tibet: Implications for the tectonic evolution of the eastern Himalaya: Lithos, v. 294–295, p. 246–262, https://doi.org/10.1016/j.lithos.2017.09.014.

Inger, S., and Harris, N., 1993, Geochemical constraints on leucogranite magmatism in the Langtang Valley, Nepal Himalaya: Journal of Petrology, v. 34, p. 345–368, https://doi.org/10.1093/petrology/34.2.345.

Kohn, M.J., Paul, S.K., and Corrie, S.L., 2010, The lower Lesser Himalayan sequence: A Paleoproterozoic arc on the northern margin of the Indian plate: Geological Society of America Bulletin, v. 122, no. 3–4, p. 323–335, https://doi.org/10.1130/B26587.1.

Le Fort, P., Cuney, M., Deniel, C., France-Lanord, C., Sheppard, S.M.F., Upreti, B.N., and Vidal, P., 1987, Crustal generation of the Himalayan leucogranites: Tectonophysics, v. 134, p. 39–57.

Lederer, G.W., Cottle, J.M., Jessup, M.J., Langille, J.M., and Ahmad, T., 2013, Timescales of partial melting in the Himalayan middle crust: insight from the

Leo Pargil dome, northwest India: Contributions to Mineralogy and Petrology, v. 166, p. 1415–1441, https://doi.org/10.1007/s00410-013-0935-9.

Mottram, C.M., Argles, T.W., Harris, N.B.W., Parrish, R.R., Horstwood, M.S. A., Warren, C.J., and Gupta, S., 2014, Tectonic interleaving along the Main Central Thrust, Sikkim Himalaya: Journal of the Geological Society, v. 171, p. 255–268, https://doi.org/10.1144/jgs2013-064.

Mottram, C.M., Parrish, R.R., Regis, D., Warren, C.J., Argles, T.W., Harris, N.B.W., and Roberts, N.M.W., 2015, Using U-Th-Pb petrochronology to determine rates of ductile thrusting: time windows into the Main Central Thrust, Sikkim Himalaya: Tectonics, v. 34, p. 1355–1374, https://doi.org/10.1002/2014TC003743.

Patiño Douce, A.E., and Johnston, A.D., 1991, Phase equilibria and melt productivity in the pelitic system: implications for the origin of peraluminous granitoids and aluminous granulites: Contributions to Mineralogy and Petrology, v. 107, p. 202–218.

Prince, C., Harris, N., and Vance, D., 2001, Fluid-enhanced melting during prograde metamorphism: Journal of the Geological Society, v. 158, p. 233–241, https://doi.org/10.1144/jgs.158.2.233.

Richards, A., Parrish, R., Harris, N., Argles, T., and Zhang, L., 2006, Correlation of lithotectonic units across the eastern Himalaya, Bhutan: Geology, v. 34, 341–344, https://doi.org/10.1130/G22169.1.

Spencer, C.J., Dyck, B., Mottram, C.M., Roberts, N.M., Yao, W.H., and Martin, E.L., 2018. Deconvolving the pre-Himalayan Indian margin–tales of crustal growth and destruction: Geoscience Frontiers, https://doi.org/10.1016/j.gsf.2018.02.007.

Spencer, C.J., Harris, R.A., and Dorais, M.J., 2012, Depositional provenance of the Himalayan metamorphic core of Garhwal region, India: Constrained by U-Pb and Hf isotopes in zircons: Gondwana Research, v. 22, p, 26–35, https://doi.org/10.1016/j.gr.2011.10.004.

Tang, M., Wang, X.L., Shu, X.J., Wang, D., Yang, T., and Gopon, P., 2014. Hafnium isotopic heterogeneity in zircons from granitic rocks: geochemical evaluation and modeling of "zircon effect" in crustal anatexis: Earth and Planetary Science Letters, v. 389, p.188-199, https://doi.org/10.1016/j.epsl.2013.12.036.